

# Proteome and phosphoproteome analysis of brown adipocytes reveals that RICTOR loss dampens global insulin/AKT signaling

Samuel W. Entwisle\*, Camila Martinez Calejman\*, Anthony S. Valente, Robert T. Lawrence, Chien-Min Hung, David A. Guertin#, Judit Villén#

\*Authors contributed equally to the work.

#Corresponding authors: David Guertin (David.Guertin@umassmed.edu) and Judit Villén (jvillen@uw.edu)

## SUPPLEMENTAL DATA

Figure S1.....	S-2
Figure S2.....	S-3
Figure S3.....	S-4
Figure S4.....	S-5
Table S1.....	S-6
Dataset S1 (Excel file description).....	S-7
Dataset S2 (Excel file description).....	S-7
Dataset S3 (Excel file description).....	S-7

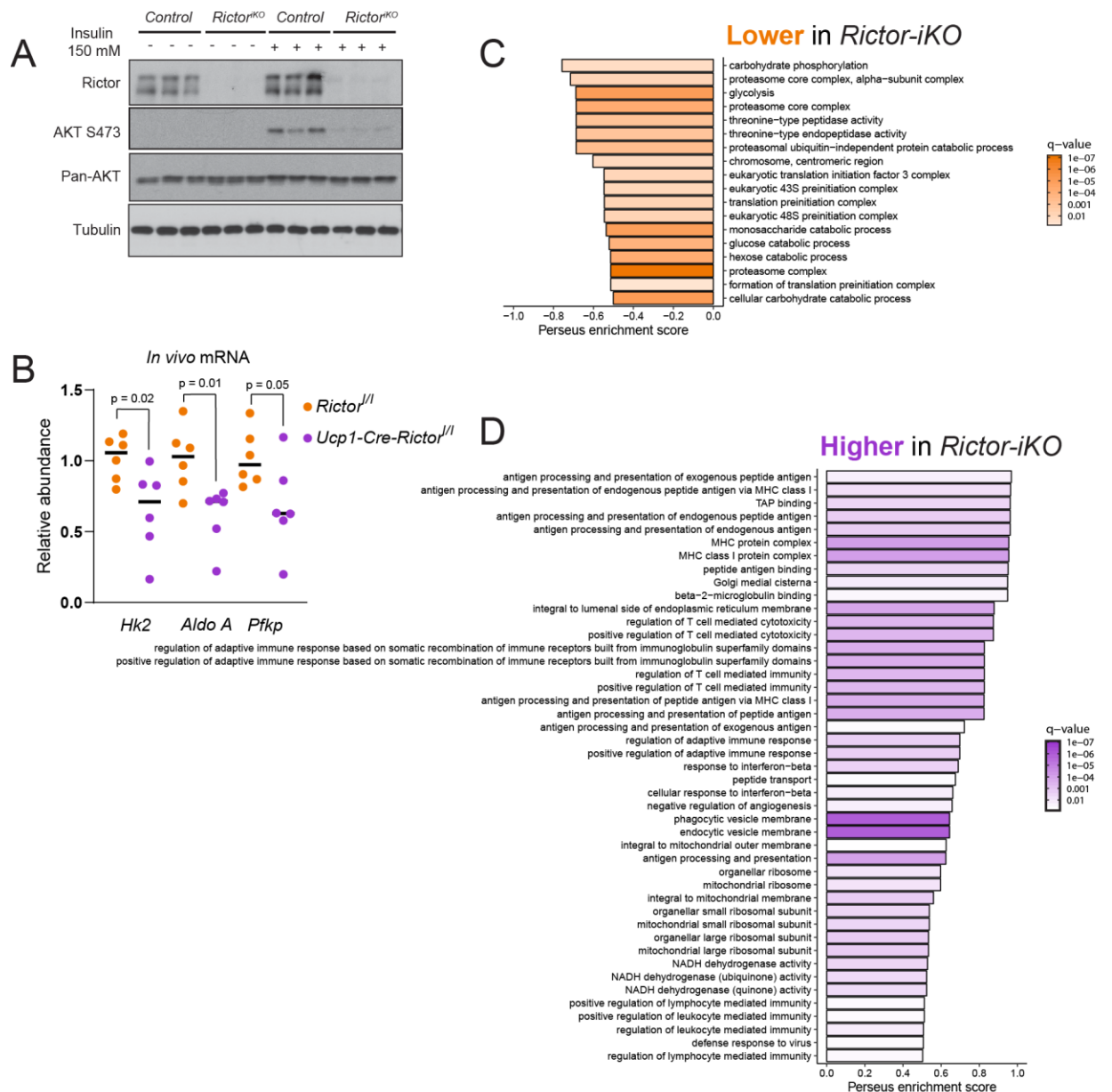


**Figure S1: Widespread proteome changes in *Rictor-iKO* brown adipocytes (related to Figure 1).** (A) Western blot showing near-complete loss of RICTOR protein in mature brown adipocytes. Pan-AKT and tubulin are protein level controls that were generated by pipetting the same relative amounts on a separate gel. (B) RT-PCR analysis of selected glycolytic genes from interscapular brown fat from *Rictor<sup>fl</sup>* (wild-type) and *Ucp1-Cre;Rictor<sup>fl</sup>* mice. (C) Complete GO enrichment results of proteins that are higher in the control versus the *Rictor-iKO*. (D) Complete GO enrichment results of proteins that are higher in the *Rictor-iKO* versus the control.

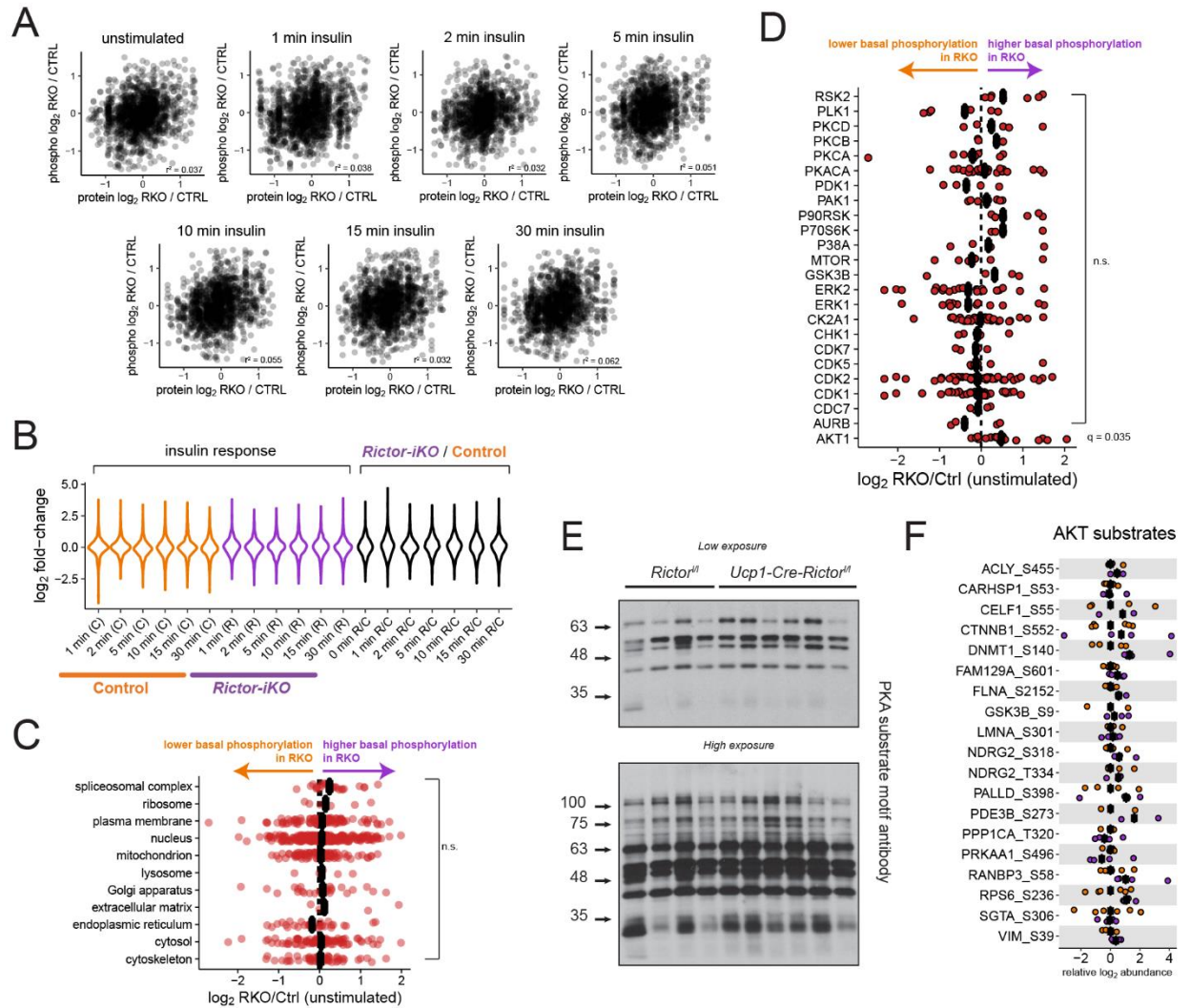


**Figure S2: Basal phosphorylation changes in *Rictor-iKO* cells (related to Figure 2).** (A) Scatter plots comparing the abundance fold-changes between *Rictor-iKO* and control, at each time point, for the proteome and phosphoproteome measurements, along with r-squared values. (B) Distributions of log<sub>2</sub> fold-changes of protein-normalized phosphorylation levels. Fold-changes were calculated between each insulin time point and untreated, in both control and *Rictor-iKO*, or between control and *Rictor-iKO* at each time point. (C) Protein-normalized phosphorylation abundance fold-changes between *Rictor-iKO* and control (all time points) for phosphorylation sites within different subcellular localization as defined by selected GO cellular component terms. (D) Protein-normalized phosphorylation abundance fold-changes between *Rictor-iKO* and control (all time points) for kinase substrate sets defined by the PhosphositePlus database<sup>28</sup>. One-sample Student's t-tests were used to assess significance in (C) and (D). (E) Western blot showing anti-PAK substrate motif antibody staining in BAT from *Rictor<sup>fl/fl</sup>* (wild-type) and *Ucp1-Cre;Rictor<sup>fl/fl</sup>* mice. Both low (top) and high (bottom) exposure images of the same blot are shown. (F) Protein-normalized quantification of annotated AKT1 or AKT2 substrates in the unstimulated condition.

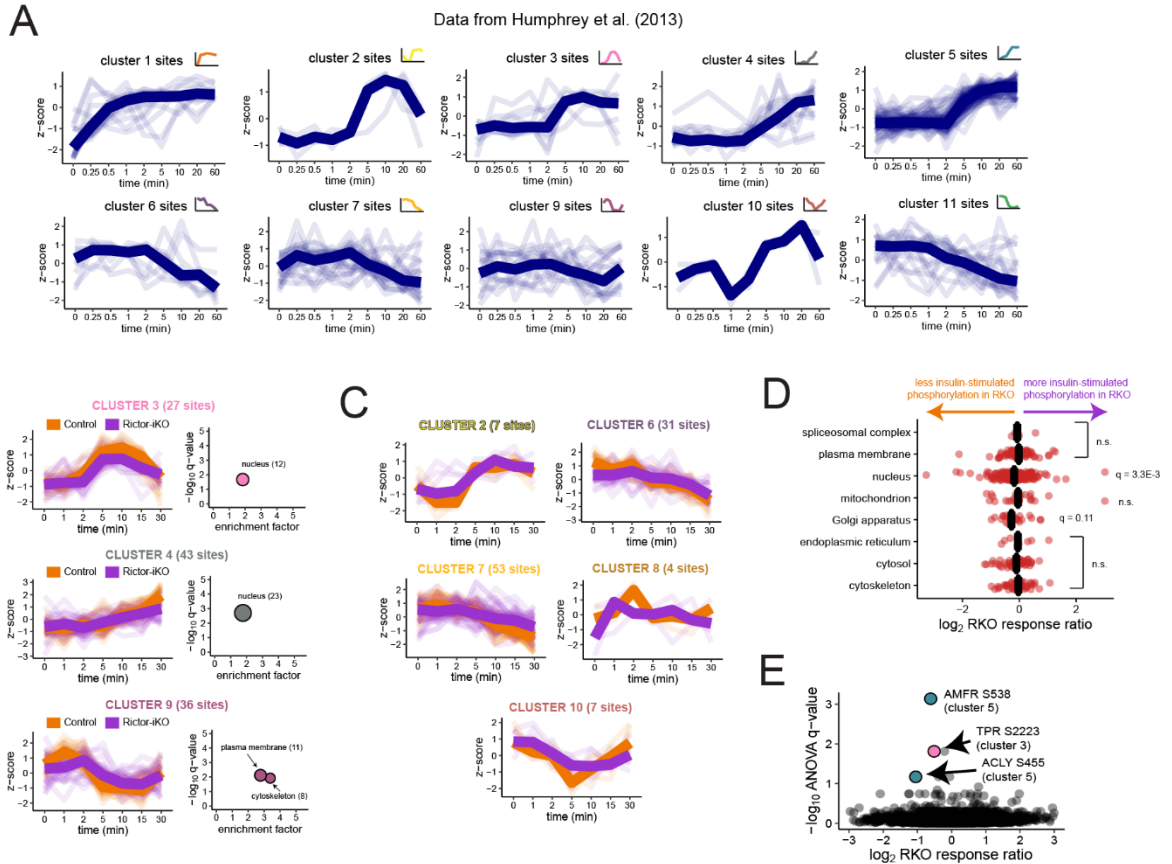


**Figure S3: Characterizing RICTOR-dependent dynamic insulin-dependent phosphorylation (related to Figure 3).** (A) Data from Humphrey et al.<sup>8</sup> were mapped to the clusters defined in Fig 3A, demonstrating consistency in the insulin temporal response between the studies. The temporal pattern of the clusters from this study are shown in the upper-right inset for each plot. (B) Average temporal response to insulin of the control and the *Rictor-iKO* for selected clusters not highlighted in Fig 3B that contained significant subcellular localization enrichments but no significant kinase-substrate enrichments. Enrichment plots (right) show fold-enrichment is plotted on the x-axis, while the y-axis contains the  $-\log_{10}$  q-value from a Fisher's Exact Test corrected by the Benjamini-Hochberg method. The size of the circles corresponds to the number of sites represented by each term. (C) Average temporal response to insulin of the control and the *Rictor-iKO* for selected clusters not highlighted in Fig 3B that contained no significant subcellular localization enrichments or kinase-substrate enrichments. (D) Log<sub>2</sub> maximum insulin fold-changes relative to t=0 in control cells for phosphorylation sites that are annotated as belonging to subcellular localizations according to GO cellular components. Only sites that significantly respond to insulin at  $q \leq 0.05$  in either control or *Rictor-iKO* cells are shown here. q-values correspond to a one-sample Student's t-test followed by a Benjamini-Hochberg correction. (E) Volcano plot showing the RKO response ratio on the x-axis, and the  $-\log_{10}$  q-value on the y-axis (2-way ANOVA corrected with the Benjamini-Hochberg method). Three notable sites are highlighted along with their clusters as defined in Fig 3A.

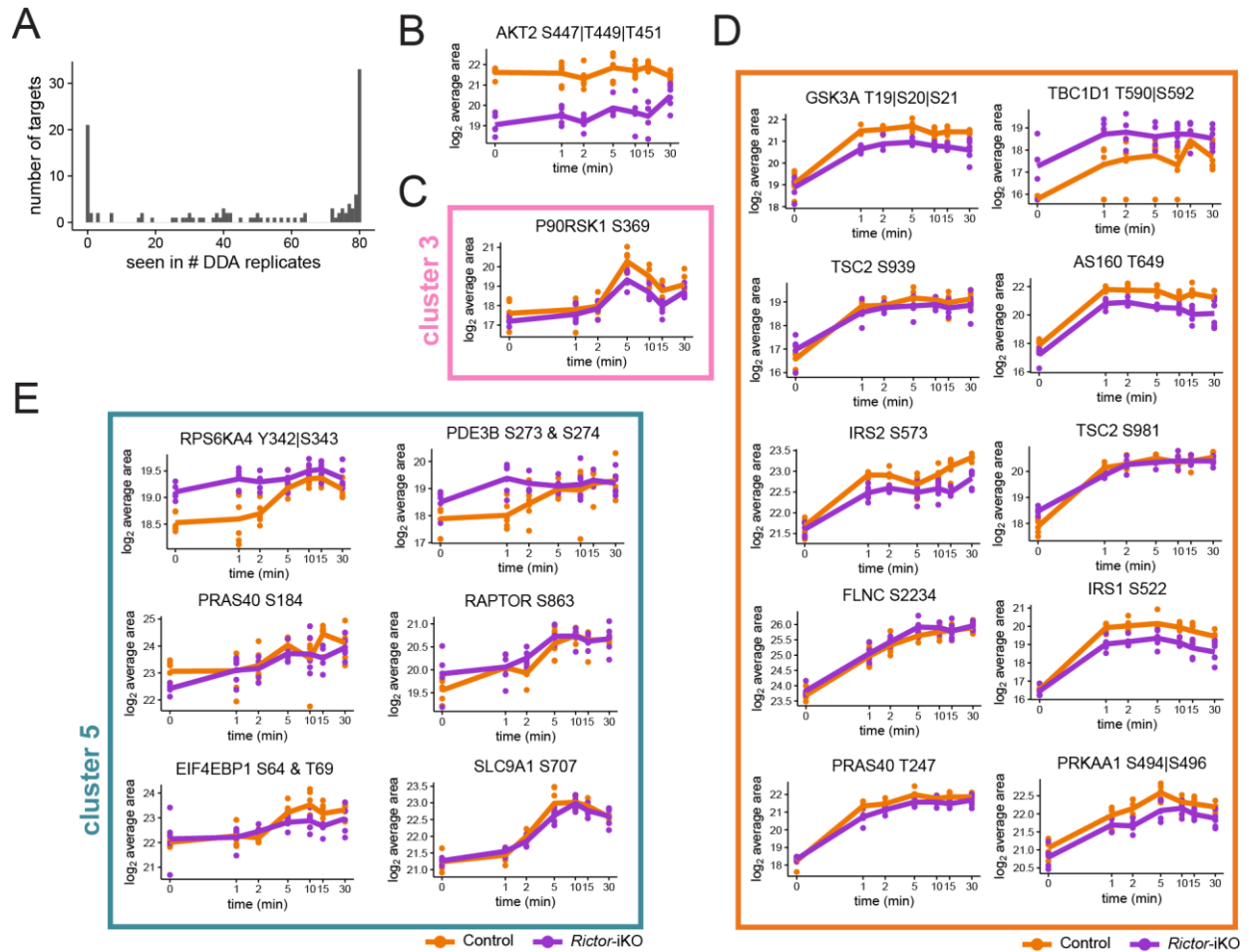


**Figure S4: RICTOR-dependence of diverse insulin-sensitive signaling nodes revealed by targeted MS (related to Figure 4). (A)** Histogram of targeted phosphopeptides according to the number of samples in which they were observed in the global phosphoproteome analysis. **(B)** Quantification of a phosphopeptide containing AKT2 turn motif phosphorylation. **(C)** Quantification of a phosphopeptide containing hydrophobic motif phosphorylation of P90RSK1. **(D-E)** Phosphopeptides corresponding to cluster 1 **(D)**, and cluster 5 **(E)** from Fig 3A.

**Table S1. Mouse primer sequences for quantitative RT-PCR analysis**

<b>Gene</b>	<b>Forward primer (5'-3')</b>	<b>Reverse primer (5'-3')</b>
<i>Tbp</i>	GAAGCTGCGGTACAATTCCAG	CCCCTTGTACCCTTCACCAAT
<i>Isg15</i>	AGACCCAGACTGGAAAGGGT	CGATTTCTGGTGTCCGTGA
<i>Ifit3</i>	AGATTTCTGAACTGCTCAGCCC	TTCCCGGTTGACCTCACTCA
<i>Stat1</i>	CCTGCGTGCAGTGATCGTTT	CAAATGCTTCCGTTCCCACG
<i>Stat2</i>	TGGGACTTCGGCTTCTTGACT	GGTACACGTACTIONCAACCACGA
<i>Ifih1</i>	CTGGGATGGACGCAGATGTT	GCAAGTGGAGACTCGTCA
<i>Pfkip</i>	AGGAGGGCAAAGGAGTGTTT	TTGGCAGAAATCTTGTTCC
<i>Aldo A</i>	TCCATTGGCACCGAGAACAC	TTGATAACTTGGGGGAAGGGA
<i>Hk2</i>	GGAACCCAGCTGTTTGACCA	CAGGGGAACGAGAAGGTGAAA

**Dataset S1: Quantification of proteins from DDA analysis of the Control and *Rictor-iKO* insulin time series.** Excel file containing the following three sheets:

- *replicates*: protein-level quantification of individual samples and time-point averages.
- *summary*: simplified table of protein-level time-point averages, statistics, and annotations.
- *key*: column descriptions.

**Dataset S2: Quantification of phosphorylation sites from DDA analysis of the Control and *Rictor-iKO* insulin time series.** Excel file containing the following five sheets:

- *replicates*: phosphorylation site-level quantification of individual samples.
- *summary*: simplified table of phosphorylation site-level time-point averages, statistics, and annotations.
- *replicates (prot-norm)*: protein-normalized, phosphorylation site-level quantification of individual samples.
- *summary (prot-norm)*: simplified table of protein-normalized, phosphorylation site-level time-point averages, statistics, and annotations.
- *key*: column descriptions.

**Dataset S3: Quantification of phosphopeptides from PRM analysis of the Control and *Rictor-iKO* insulin time series.** Excel file containing the following three sheets:

- *replicates*: phosphopeptide-level quantification of individual samples.
- *summary*: simplified table of phosphopeptide-level time-point averages, statistics, and annotations.
- *key*: column descriptions.